Do Columnar Defects Produce Bulk Pinning?

M. V. Indenbom,[1,2] C. J. van der Beek,[1] M. Konczykowski,[1] and F. Holtzberg[3]
[1]*Laboratoire des Solides Irradiés, Ecole Polytechnique, 91128 Palaiseau, France*
[2]*Institute for Solid State Physics R.A.S., 142432 Chernogolovka, Moscow district, Russia*
[3]*Emeritus, IBM Thomas J. Watson Research Center, Yorktown Heights, New York 10598*
(Received 24 November 1998)

From magneto-optical imaging performed on heavy-ion-irradiated $YBa_2Cu_3O_{7-\delta}$ single crystals, it is found that at fields and temperatures where strong single vortex pinning by individual irradiation-induced amorphous columnar defects is to be expected, vortex motion is limited by the nucleation of vortex kinks at the specimen surface. In the material bulk, vortex motion occurs through (easy) kink sliding. Depinning in the bulk determines the screening current only at fields comparable to or larger than the matching field, at which the majority of vortices is not trapped by an ion track.

PACS numbers: 74.60.Ec, 74.60.Ge, 74.60.Jg

Columnar defects created by heavy-ion irradiation provide very efficient vortex pinning in high temperature superconductors [1]. Nevertheless, because the column radii are very homogeneous over their length [2], it is not clear how the motion of even slightly misaligned vortices can be inhibited. Misalignment between vortices and columns may arise from the presence of the shielding current itself, since the latter implies not only a gradient of the vortex density but also vortex line curvature. The problem is illustrated in Fig. 1. If the vortex lines are inclined with respect to the ion tracks, vortex kinks connecting segments trapped by the columns can easily slide along them. The force opposing this motion is determined by the background pinning by point defects. Hence, the critical current will be orders of magnitude lower than that corresponding to the depinning of vortices from the columns by a (double) kink nucleation process [3]. The large observed critical currents [1], as well as the moderate anisotropy for vortex motion within and across the plane containing the irradiation direction and the c axis in obliquely irradiated $DyBa_2Cu_3O_{7-\delta}$ single crystals [4], indicates that kink sliding cannot be the main mechanism limiting flux motion in type-II superconductors with correlated disorder. Rather, in crystals of thickness d much greater than the penetration depth λ, it is the nucleation of vortex kinks at the crystal surface that should play this role (shaded arrow in Fig. 1) [4]. By consequence, the critical current only flows in a surface layer of thickness $\sim\lambda$; kink sliding causes the current density $j(z)$ in the bulk to drop to a value that is too small to induce vortex-kink or half-loop nucleation.

In this Letter, it is verified that vortex motion in irradiated $YBa_2Cu_3O_{7-\delta}$ (YBCO) single crystals indeed proceeds through the "hard" nucleation of kinks at the surface followed by "easy" kink sliding into the crystal bulk, *irrespective of the relative alignment between vortex lines and ion tracks*. Our method relies on the measurement of the thickness dependence of the crystals' self-field: if the critical current flows only within a surface layer, the integrated shielding current $J = \int_{-d/2}^{d/2} j(z)\,dz$, and hence the hysteretic parts of the magnetic moment and of the induction measured at the crystal surface should be independent of the thickness.

The most reliable way to demonstrate a thickness (in)dependence of the self-field, excluding the usual scatter of the crystal properties, is to observe the flux penetration into a flat sample with big surface steps. Supposing that the bulk current j is homogeneous, the characteristic field for penetration of perpendicular flux into a flat superconducting plate is proportional to $J = jd$ [5]; a much easier flux penetration into the thinner parts of such superconducting samples has clearly been observed using magneto-optics [6,7]. For surfacelike pinning, in which only a surface current J_s is present, $J = 2J_s$ and flux penetration should be like that into a crystal of constant thickness.

YBCO single crystals were grown in Au crucibles and annealed in oxygen in Pt tubes as described elsewhere [8]. For our experiments we have selected crystals with pronounced as-grown surface steps, in order to have a thickness variation of at least a factor of 2 over the crystal length. Microscopic observations in reflected polarized light revealed all crystals to be twinned [Figs. 2(a), 3(a), and 3(b)]. The crystals were irradiated at GANIL

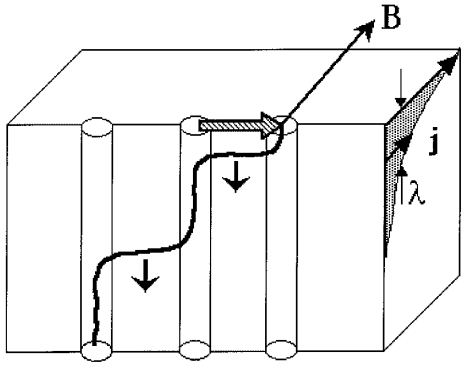

FIG. 1. Surface depinning of a vortex (bold line) from the columnar defects (cylinders). Short arrows indicate the vortex kink sliding down from the surface, producing a vortex drift to the right. The surface critical current distribution in the λ layer is sketched on the right hand "crystal face."

 0031-9007/00/84(8)/1792(4)$15.00

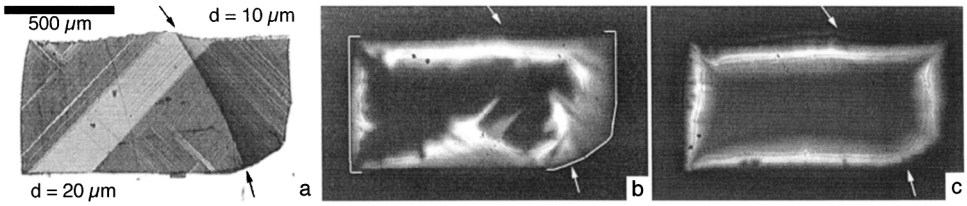

FIG. 2. Regularization of flux penetration by heavy ion irradiation. (a) Reflected polarized light photograph of the surface of a YBCO single crystal. The crystal has a large surface step (indicated by arrows), dividing it into right hand and left hand parts of thickness 10 and 20 μm, respectively. (b) and (c) show the remanent induction on the crystal surface after the application and removal of a field $H_a = 360$ G $\| c \|$ ion tracks: (b) before irradiation, $T = 40$ K; (c) after irradiation with 6 GeV Pb ions, $T = 80$ K. The arrows indicate the position of the step.

in Caen, France, using a beam of 6 GeV Pb ions oriented parallel to the crystalline c axis. The track density $n_d = 5 \times 10^{10}$ cm^{-2} corresponds to the irradiation dose and determines the matching field $B_\phi = \Phi_0 n_d = 10$ kG (Φ_0 is the flux quantum). Flux penetration before and after the irradiation was studied by means of the magneto-optical imaging technique using ferrimagnetic garnet indicators with in-plane anisotropy [9]. On all images of the flux distribution presented here the higher value of the image intensity corresponds to the higher value of the local induction.

In Fig. 2 we present images of the flux penetration into one of the crystals before and after the irradiation. This crystal has one large surface step, separating it into two parts of thickness 10 and 20 μm, respectively. Figure 2(b) shows the remanent induction before the irradiation, after the application and removal of an applied field $H_a = 360$ G $\| c$ at $T = 40$ K. Owing to the crystal's twin structure, flux penetration before the irradiation is rather irregular. This irregularity was observed in all other crystals. Nevertheless, flux penetration into the thin right hand side (denoted in the figure by the white bracket) is clearly easier than that into the thick left hand part (also with bracket) of the crystal, which has a similar twin structure.

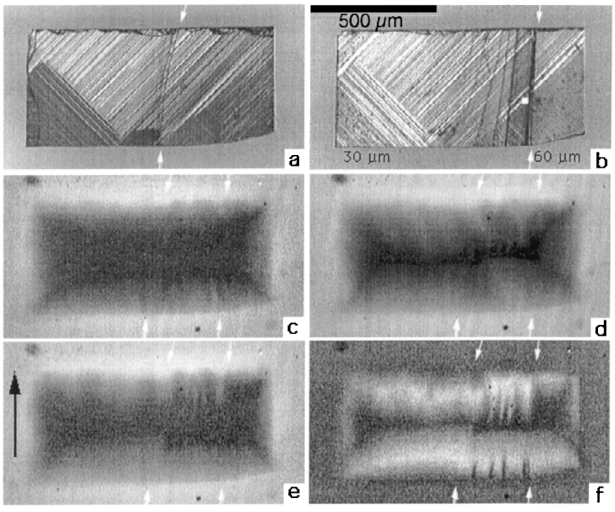

FIG. 3. Role of surface steps in the flux penetration into an YBCO crystal with columnar defects: (a) Top surface of a crystal with a 15 μm step crossing it in the center (at the arrows). (b) Mirror image of the bottom surface, with one large 10 μm step at the very right (see arrows) and a number of smaller steps. The crystal thickness monotonically increases from left to right. (c),(d) Homogeneous flux penetration into the zero-field-cooled crystal ($T = 85$ K). (c) $H_a = 177$ G; (d) $H_a = 359$ G ($\| c \|$ ion tracks). (e),(f) Image of the perpendicular induction on the crystal top surface, after cooling to 85 K in a constant in-plane field $H_\| = 80$ G applied in the direction of the bold arrow, and the subsequent application of $H_\perp = 169$ G (e), and (f) a reduction of $H_\perp$ to 84 G after application of 253 G.

The irradiation drastically changes the flux penetration pattern. Because of the very substantial increase in shielding current, the temperature had to be increased to 80 K in order to observe penetration over a distance comparable to that before irradiation [Fig. 2(c)]. Pinning by columnar defects is seen to dominate all other pinning: if any influence of the twin boundaries on the flux penetration is present, it can no longer be discerned [4]. More important, flux now penetrates *equally far into the thick and thin parts of the crystal* in accordance with the hypothesis of surface depinning.

This finding is corroborated by measurements on a second sample, cut from another irradiated crystal in such a manner as to have a series of surface steps of the same sign, oriented perpendicularly to its longer sides. Figures 3(a) and 3(b) show that this sample has a big step of height ~ 15 μm on the top surface, dividing it into two roughly equal parts of thickness 30 and 50–60 μm, respectively. On the bottom surface [the mirror image of which is shown in Fig. 3(b)], there is another large step of height ~ 10 μm, together with a number of smaller steps of height ~ 1 μm. The twin patterns revealed in reflected polarized light are equivalent on both crystal sides and are not interrupted by the steps, thus showing the perfect continuity of the sample. Subsequent magneto-optical imaging of the flux distribution was carried out on the top surface. Again applying a field parallel to the columnar defects, i.e., perpendicular to the plane of the zero-field cooled sample, we observed the same striking phenomenon: the flux penetration pattern appears as if the crystal had constant thickness [Figs. 3(c) and 3(d)]. The distance over which flux penetrates is the same along all the sample edges, i.e., *J is thickness independent*. The small irregularities in flux penetration at the upper edge in Fig. 3(d) may be ascribed to the defects caused by cutting [seen in Fig. 3(a)].

The above result constitutes strong evidence in favor of the model in which depinning of vortices from parallel columnar defects is limited by the nucleation of vortex kinks at both crystal surfaces, the critical current being the surface current necessary for this process [Fig. 4(a)]. Vortex depinning in the situation where the field is applied parallel to the columns thus resembles depinning in the case where either are misaligned [4]. Simultaneously, it is a well-known fact that the magnetic moment of heavy-ion irradiated YBCO rapidly decreases when the angle between the applied field and the columns is increased [1]. It is therefore interesting to learn how tilting the field affects surface depinning. For this, the same crystal was cooled in a field $H_{\parallel} = 80$ G directed parallel to the crystal plane and parallel to its shorter sides [as indicated in Fig. 3(e)]. The in-plane field was not changed during the subsequent application of a perpendicular field $H_{\perp}$. Although the penetration of $H_{\perp}$ appeared to be somewhat more pronounced in the thinner left hand part of the crystal [Fig. 3(e)], the difference in penetration depth between the two parts was considerably less than what should be expected for bulk pinning, would this have been relevant after relieving the vortex confinement to the columnar defects.

We also observe an intriguing easy flux motion along the small surface steps on the bottom face of the crystal. Such a pronounced influence of these steps is not to be expected in case bulk pinning is dominant. The perpendicular induction (directed towards the observer) clearly penetrated further along the steps at the upper edge [Fig. 3(e)]. When the applied field was reduced, flux left the crystal preferentially at the lower edge, while the features arising from the earlier preferential penetration at the upper edge remained frozen [Fig. 3(f)]. Reversing the sign of either $H_{\perp}$ or $H_{\parallel}$ reversed the sense of easy flux motion along the steps: flux now penetrated preferentially at the lower edge in increasing $H_{\perp}$ and at the upper edge in decreasing $H_{\perp}$.

The motion of inclined vortices is mediated by *unidirectional* kink sliding from the surface with leading vortex end, where kinks nucleate, to the opposite surface [see Fig. 4(b)]. The observed easy flux penetration along the sharp small steps on the bottom surface of the crystal is a result of easy kink nucleation at these steps. The big step on the top face is smooth and does not affect surface kink nucleation. The need to nucleate the kinks on one surface restricts only the critical current flow to this surface (cf. Fig. 4), which explains the fact that inclined vortices penetrate the crystal approximately twice as far for the same temperature and $H_{\perp}$, as well as the rapid decrease of the sample magnetic moment when the applied field is tilted from the track direction. The strong sensitivity to surface defects is another fact supporting the idea of surfacelike pinning: as in the case of the Bean-Livingston surface barrier [10] the nucleation of vortex kinks is considerably facilitated by small but sharp surface irregularities.

Unfortunately, the magneto-optical technique is limited to low fields. In order to extend the measurements to fields comparable to B_{ϕ} we used the micro-Hall-probe technique [11]. A small homemade single crystalline InSb Hall probe with active area $\approx 80 \times 80\ \mu\text{m}^2$ was consecutively placed in equivalent positions on the thick and thin parts of the crystal shown in Fig. 3, such that in each case its distance to the crystal ends was approximately equal to half the crystal width. Loops of the hysteretic induction B_H were measured for applied fields up to 50 kG and temperatures $45 < T < 85$ K. Figure 5 shows the difference $\Delta B = B_H - H_a$ measured on both the thick and the thin parts of the crystal at $T = 60$ and 80 K, as a function of the local value of B_H. The shape of these loops is in good agreement with those in the literature [1]. It is seen that at low field ($B_H < 2$ kG and $B_H < 500$ G for $T = 60$ and 80 K, respectively) the "local magnetization" ΔB measured on the thick and thin parts of the crystal *practically coincides* or differs by less than the amplitude of the low field ΔB irregularities. This contradicts the ratio of ≈ 2 expected from the thickness variation for the case of bulk pinning and confirms the magneto-optical

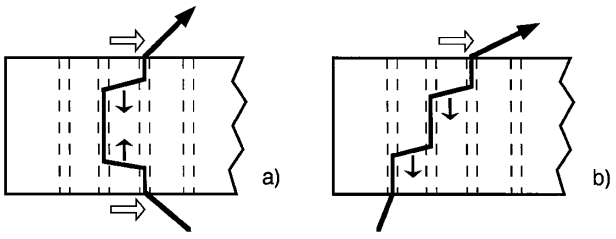

FIG. 4. Vortex kink motion in perpendicular field (a) and inclined field (b). (a) Kinks nucleate at both crystal surfaces, slide into the interior and anihilate there with each other—the critical current of kink nucleation flows on the both surfaces. (b) Unipolar kinks nucleate at the vortex "leading head" and move down to the opposite crystal surface—the critical current flows on the upper surface only.

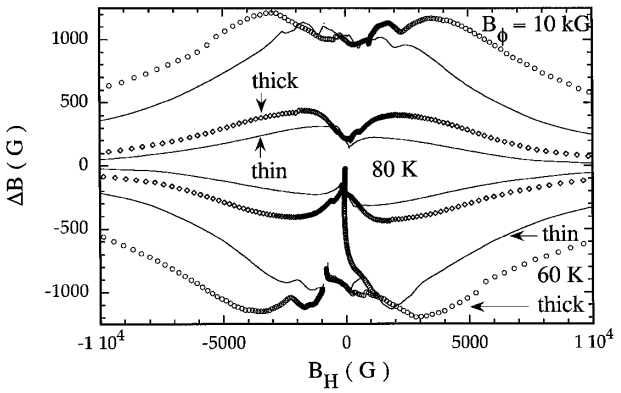

FIG. 5. Local "magnetization" loops $\Delta B = B_H - H_a$, measured on the crystal shown in Fig. 3 at 60 and 80 K. Open symbols and thin lines represent data taken on the thick and thin parts of the crystal, respectively. The conditions of the magneto-optical experiments are reproduced by the virgin magnetization curve and subsequent low field data, which show a near overlap of the "thick" and "thin" data up to $B_H \approx 2$ kG for $T = 60$ K and up to 500 G for $T = 80$ K.

observations. This field interval, in which vortex motion is limited by kink nucleation at the surface, corresponds to the regime where the width of the magnetic hysteresis loop shows a plateau ($T \lesssim 55$ K), or increases with field ($T \gtrsim 55$ K). The loops start to deviate from each other at the induction $B_{\max}$ where $|\Delta B|$ measured on the thinner part is maximum. A comparison with the virgin B_H curve shows that $B_{\max}$ is greater than the field of full flux penetration. Above $B_{\max}$, ΔB decreases until, for $B_H \gtrsim B_\phi$, ΔB remains constant and displays the thickness dependence characteristic for bulk pinning.

We interpret the occurrence of either surface or bulk depinning in the different regimes of the magnetic hysteresis loop in terms of pinning of single vortices by individual columns at low fields (each vortex can find an empty track) and plastic vortex creep at higher fields $\gtrsim B_\phi$. The single-vortex pinning regime corresponds to that of surface depinning. In this regime, the critical current should be estimated as $j_c \sim \Delta B/\mu_0\lambda$, instead of the usual $j_c \sim \Delta B/\mu_0 d$. This yields a critical current value $j_c \gtrsim 10^8$ A cm^{-2} for single vortex depinning from a track, which at low T tends to the initial estimates which had j_c comparable to the depairing current [12]. It is clear that with such current values, the usual critical state in the crystal bulk cannot exist: the self-field would generate large vortex curvature and many "preformed" vortex kinks that would immediately slide to the crystal equator and mutually annihilate. Thus bulk pinning can appear at fields only when single-vortex pinning is no longer relevant. This happens when H_a approaches a sizable fraction of B_ϕ: many free vortices appear in the system, as was directly observed by scanning tunneling microscopy [13] and revealed by model calculations [14]. In this case the plastic motion of these free vortices through the "forest" of vortices trapped by the columnar defects determines the critical current and the screening properties of the superconductor. Although much lower than the current needed for depinning from a track, this critical current is still much higher than that of the unirradiated crystal [3,15].

In conclusion, in order to depin vortices that are trapped along their entire length by columnar traps, it suffices to nucleate vortex kinks at the sample surface only; further depinning occurs by kink sliding. The observed thickness independence of the shielding current in YBCO crystals with parallel columnar defects ($\| c$) proves that the critical current is that necessary for kink nucleation, and flows only on the surface. Surface imperfections can considerably facilitate the nucleation process; sharp surface steps induce a diodelike flow of vortices which should also be seen as an asymmetry of the magnetization loops [16]. Similar gigantic surface pinning may be expected for pinning by twin planes and for intrinsic pinning.

We gratefully acknowledge S. Bouffard for the help with the irradiation and Th. Schuster for discussions on the central idea of the present work.

[1] L. Civale *et al.*, Phys. Rev. Lett. **67**, 648 (1991); M. Konczykowski *et al.*, Phys. Rev. B **44**, 7167 (1991); V. Hardy *et al.*, Physica (Amsterdam) **201C**, 85 (1992); M. Leghissa *et al.*, Europhys. Lett. **11**, 323 (1992).
[2] V. Hardy *et al.*, Nucl. Instrum. Methods Phys. Res., Sect. B **54**, 472 (1991); B. Holzapfel *et al.*, J. Alloys Compd. **195**, 411 (1993).
[3] D. R. Nelson and V. M. Vinokur, Phys. Rev. Lett. **68**, 2398 (1992); Phys. Rev. B **48**, 13 060 (1993).
[4] Th. Schuster *et al.*, Phys. Rev. B **50**, 9499 (1994); Th. Schuster *et al.*, Phys. Rev. B **51**, 16 358 (1995); Th. Schuster *et al.*, Phys. Rev. B **53**, 2257 (1996).
[5] D. J. Frankel, J. Appl. Phys. **50**, 5402 (1979); M. Däumling and D. C. Larbalestier, Phys. Rev. B **40**, 9350 (1989); L. W. Conner and A. P. Malozemoff, Phys. Rev. B **43**, 402 (1991); E. H. Brandt and M. V. Indenbom, Phys. Rev. B **48**, 12 893 (1993).
[6] Th. Schuster *et al.*, Phys. Rev. B **50**, 16 684 (1994).
[7] Th. Schuster *et al.*, Phys. Rev. B **52**, 10 375 (1995).
[8] F. Holtzberg and C. Feild, Eur. J. Solid State Inorg. Chem. **27**, 107 (1990).
[9] L. A. Dorosinskii *et al.*, Physica (Amsterdam) **203C**, 149 (1992); M. R. Koblischka and R. J. Wijngaarden, Supercond. Sci. Technol. **8**, 199 (1995).
[10] C. P. Bean and J. D. Livingston, Phys. Rev. Lett. **12**, 14 (1964).
[11] M. Konczykowski, F. Holtzberg, and P. Lejay, Supercond. Sci. Technol. **4**, S331 (1991).
[12] E. H. Brandt, Phys. Rev. Lett. **69**, 1105 (1992).
[13] S. Behler *et al.*, Phys. Rev. Lett. **72**, 1750 (1994).
[14] C. Reichhardt *et al.*, Phys. Rev. B **53**, R8898 (1996); C. A. Mair, Master's thesis, Vrije Universiteit, Amsterdam, 1998.
[15] L. Radzihovsky, Phys. Rev. Lett. **74**, 4923 (1995); C. Wengel and U. C. Täuber, Phys. Rev. Lett. **78**, 4845 (1998).
[16] M. Konczykowski *et al.*, Physica (Amsterdam) **282C–287C**, 2189 (1997).